APPLIED AND ENVIRONMENTAL MICROBIOLOGY, Dec. 1997, p. 4770–4777 Vol. 63, No. 12
0099-2240/97/$04.00+0

Electrostatic Interactions, but Not the YGNGV Consensus Motif, Govern the Binding of Pediocin PA-1 and Its Fragments to Phospholipid Vesicles†

YUHUAN CHEN, RICHARD D. LUDESCHER, AND THOMAS J. MONTVILLE*

Department of Food Science, Cook College, Rutgers, The State University of New Jersey, New Brunswick, New Jersey 08901-8520

Received 18 June 1997/Accepted 26 September 1997

The purpose of this study was to characterize in detail the binding of pediocin PA-1 and its fragments to target membranes by using tryptophan fluorescence as a probe. Based on a three-dimensional model (Y. Chen, R. Shapira, M. Eisenstein, and T. J. Montville, Appl. Environ. Microbiol. 63:524–531, 1997), four synthetic N-terminal pediocin fragments were selected to study the mechanism of the initial step by which the bacteriocin associates with membranes. Binding of pediocin PA-1 to vesicles of phosphatidylglycerol, the major component of *Listeria* membranes, caused an increase in the intrinsic tryptophan fluorescence intensity with a blue shift of the emission maximum. The Stern-Volmer constants for acrylamide quenching of the fluorescence of pediocin PA-1 in buffer and in the lipid vesicles were 8.83 ± 0.42 and 3.53 ± 0.67 M^{-1}, respectively, suggesting that the tryptophan residues inserted into the hydrophobic core of the lipid bilayer. The synthetic pediocin fragments bound strongly to the lipid vesicles when a patch of positively charged amino acid residues (K-11 and H-12) was present but bound weakly when this patch was mutated out. Quantitative comparison of changes in tryptophan fluorescence parameters, as well as the dissociation constants for pediocin PA-1 and its fragments, revealed that the relative affinity to the lipid vesicles paralleled the net positive charge in the peptide. The relative affinity for the fragment containing the YGNGV consensus motif was 10-fold lower than that for the fragment containing the positive patch. Furthermore, changing the pH from 6.0 to 8.0 decreased binding of the fragments containing the positive patch, probably due to deprotonation of His residues. These results demonstrate that electrostatic interactions, but not the YGNGV motif, govern pediocin binding to the target membrane.

Bacteriocins from lactic acid bacteria are similar to other antimicrobial peptides in nature that form poration complexes in the target cell's membrane (23, 34, 36). The practical aspects (19, 21, 30, 31, 33, 35, 40, 43) and the basic biochemical and genetic elements involved in bacteriocin biosynthesis have been extensively explored due to the well-documented lethal activity of bacteriocins against food-borne pathogens (for reviews, see references 1, 2, 22, and 32). Klaenhammer's classification of bacteriocins into four groups (23) provides one useful schema within which to compare properties of various bacteriocins. The mechanistic action of nisin, a lanthionine-containing class I bacteriocin commercially available worldwide, is the most thoroughly studied action. Highly defined in vitro systems consisting of lipid vesicles derived from a sensitive microorganism (44), synthetic phospholipid vesicles or planar bilayers (13, 16, 18), phospholipid monolayers (12), or detergent micelles (41) have been used to investigate how nisin molecules interact with membranes. Studies with nisin variants and fragments suggest that different domains of the nisin molecule are essential for binding, pore formation, and biological activity. While the N-terminal domain remains at the surface of the membrane, the C-terminal domain of the nisin molecule inserts into the hydrophobic region of the lipid bilayer (5, 17, 18, 27).

Much less is known about how class II bacteriocins interact with the membranes of sensitive microorganisms. Pediocin PA-1 is a representative member of the class IIa bacteriocins, which are *Listeria*-active, heat-stable peptides containing a YGNGV consensus amino acid motif in the N-terminal region (23). In general, the 44-amino-acid molecule pediocin PA-1 acts at the target cell's membrane through a multistep process consisting of binding, insertion, and pore formation, a mechanism shared by most bacteriocins from lactic acid bacteria (1, 2, 9). As the first step in the functioning of pediocin PA-1, binding of the bacteriocin to the membrane is a prerequisite for subsequent insertion and pore formation that leads to cell death. Pediocin PA-1 interacts directly with lipid vesicles composed of *Listeria monocytogenes* total lipids and permeabilizes the membrane lipid matrix without a requirement for a protein receptor (7, 8). This is not inconsistent with the requirement for a protein receptor for in vivo activity suggested by Chikindas et al. (9), since such a receptor may facilitate the postbinding steps of insertion, aggregation, and pore formation. The proposed receptor, however, is clearly not absolutely essential for pediocin PA-1 binding in vitro. The mechanism for the initial pediocin-membrane binding remains poorly understood. A structural model for pediocin PA-1 (8) predicts that 18 amino acids in the N-terminal part of the peptide assume a three-strand β-sheet conformation. The tip of the β-hairpin connecting the second and third strands contains two positively charged residues (termed the positive patch) potentially important in bacteriocin binding, and the N-terminal β-turn between the first and second strands contains the YGNGV consensus motif. The function of this consensus motif is unknown, but it is hypothesized that this region is the peptide domain

* Corresponding author. Phone: (732) 932-9611, ext. 218. Fax: (732) 932-6776. E-mail: montville@aesop.rutgers.edu.

† Report D-10580-1-97 of the New Jersey Agricultural Experiment Station.

TABLE 1. Primary sequence of pediocin PA-1 and N-terminal fragments[a]

Peptide	Amino acid sequence
Pediocin PA-1	KY**YGNGV**TCGKHSCSVDWGKATTCIINNGAMAWATGGHQGNHKC
Pediocin N15	WK**YGNGV**TCGKHSCS
Pediocin N7	WK**YGNGV**
Pediocin N8-15	WTCGKHSCS
Pediocin N^m8-15	WTCGILSCS

[a] Single-letter codes of amino acids are used; positively charged residues are underlined, and the consensus motif is in boldface type.

involved in recognition of target membranes by *Listeria*-active bacteriocins (2, 4, 23).

Native pediocin PA-1 contains two tryptophan residues (20) whose intrinsic fluorescence can be followed spectroscopically to generate information at the molecular level about how the peptide binds to the membrane. Tryptophan fluorescence emission spectral parameters change with the polarity of the environment so that tryptophan residues bound to membranes can be differentiated from the tryptophans of peptide molecules in aqueous solution (6, 38, 39). Genetically engineered nisin and chemically synthesized magainin containing an introduced tryptophan residue have been used to elucidate binding and insertion mechanisms of nisin (17, 27) and magainin 2 (28).

The purpose of this study was to obtain a detailed understanding of how pediocin PA-1 binds to the membrane in the absence of a protein receptor. Specifically, we examined the relationship between pediocin PA-1's structure and function and used tryptophan fluorescence as a probe to demonstrate the role of the positively charged residues in the β-hairpin loop in bacteriocin binding to phospholipid vesicles.

MATERIALS AND METHODS

Preparation of pediocin PA-1 and pediocin fragments. To obtain full-length, native pediocin PA-1, *Pediococcus acidilactici* PAC 1.0 was grown in lactobacillus MRS broth supplemented with 0.6% yeast extract at 30°C for 20 to 22 h. Culture supernatant was collected, and pediocin PA-1 was purified to homogeneity as previously reported (8). To investigate more thoroughly the role of specific amino acid residues, structural features predicted by the three-dimensional model (8) were examined to identify four pediocin fragments of interest. These were then chemically synthesized (Bio Synthesis, Inc., Lesisville, Tex.). The fragments designated pediocin N15, pediocin N7, and pediocin N8-15 contained, respectively, all 15 residues, the first 7 residues, and residues 8 to 15 of the 15 amino acids of the N-terminal sequence but had an introduced tryptophan as residue 1 which served as the probe (Table 1). A mutant fragment, pediocin N^m8-15, had the same sequence as pediocin N8-15, except that charged residues K-11 and H-12 were replaced with Ile and Leu, respectively. A disulfide bond probably exists between C-9 and C-14 in the candidate pediocin fragments since spontaneous formation of intrapeptide disulfide bonds occurs in synthetic pediocin-like bacteriocins (15). Pediocin N^m8-15 was resuspended in 2-(*N*-morpholino)ethanesulfonic acid (MES) (50 mM pH 6.0) buffer containing 60% ethanol, and all of the other pediocin fragments were resuspended in 50 mM MES buffer (pH 6.0). Peptide concentrations were determined by measuring A_{280} with a spectrophotometer (model UV160; Shimadzu Scientific Instruments, Columbia, Md.). The activities of pediocin PA-1 and the fragments were determined by the spot-on-the-lawn assay by using *L. monocytogenes* Scott A as the indicator (35).

Preparation of lipid vesicles. A highly defined membrane model system was used to study pediocin binding. Large unilamellar vesicles were made by using the extrusion method described by MacDonald et al. (26). Dimyristoyl-phosphatidylglycerol (Avanti Polar Lipids, Alabaster, Ala.) was used to make the vesicles, since anionic phospholipids are the major component of the *L. monocytogenes* Scott A membrane (10, 44). Moreover, the majority of the fatty acids associated with the *Listeria* phospholipids are myristic (14:0) and palmitic (16:0) fatty acids with a methyl group attached to the second or third carbon from the end of the acyl chain (29). In some experiments, total lipids were extracted from *L. monocytogenes* cells (8) and used. To make the lipid vesicles, lipid dissolved in chloroform was dried under a stream of N_2 gas in a siliconized microcentrifuge tube, and the residual solvent was removed by centrifugation under a vacuum for 2 h. The dried lipid was resuspended in MES buffer (50 mM, pH 6.0). The suspension was vortex mixed and subjected to five freeze-thaw cycles in a solid CO_2-ethanol bath to form multilamellar vesicles. By using a Liposofast microextruder (Avestin, Ottawa, Canada), the multilamellar vesicle mixture was successively extruded through polycarbonate filters (Poretics, Livermore, Calif.) with 0.6-μm pores five times and with 0.2-μm pores five times and then through two (stacked) filters with 0.1-μm pores 21 times. Lipid vesicles prepared by this method were homogeneous in size with an average diameter close to 100 nm (26). The lipid vesicles were kept on ice for up to 3 h until they were used.

Pediocin binding measurements and analysis. Binding of pediocin PA-1 and its fragments was determined by following changes in the fluorescence of tryptophan residues when the peptides were exposed to the large unilamellar vesicles. Tryptophan fluorescence was measured with a spectrofluorometer (model F1T11; Spex Industries, Metuchen, N.J.). Emission spectra over the range from 290 to 450 nm were determined upon excitation at 280 nm and with excitation and emission slit settings of 4 nm. Briefly, small quantities (5, 10, 20, 30, and 50 μl) of a stock lipid suspension (11.6 mM) were sequentially added to a fixed concentration (3.8 μM for the native pediocin, 7.2 to 11.0 μM for the fragments) of pediocin solution in 2.0 ml of MES buffer (50 mM at an appropriate pH). The peptide-lipid mixtures were stirred constantly in cuvettes, and the fluorescence emission spectra were recorded for the peptide alone and for each lipid addition. The emission spectrum for a given ratio of lipid concentration to peptide concentration obtained after 1 min of incubation was similar to that obtained after 4 min of incubation, suggesting that equilibrium was reached rapidly. The baseline fluorescence contributed by buffer or the lipid vesicles in the absence of peptides was subtracted from each fluorescence spectrum. As a control, the fluorescence emission for the tryptophan derivative *N*-acetyltryptophanamide in MES buffer (50 mM, pH 6.0) was also determined.

Several steps were performed to generate binding constants. Each tryptophan emission spectrum was analyzed to determine the maximum emission wavelength (λ_{max}) and the fluorescence intensity (I). The intensity value was obtained by integrating the emission curve and was corrected for dilution effects. Fluorescence titration curves relate blue shift ($\Delta\lambda_{max} = \lambda_{max_o} - \lambda_{max}$, in nanometers), relative blue shift ($\lambda_{max_o}/\lambda_{max}$), or relative intensity increase (I/I_o) to total lipid concentrations, where the subscript o denotes the parameter in the absence of lipid vesicles. The titration curves were analyzed by using the following equation (3, 27, 39):

$$\varepsilon - 1 = (\varepsilon_b - 1) - (K_d/n)\,(\varepsilon - 1)/m \quad (1)$$

where K_d, n, and m are the dissociation constant of a lipid-peptide complex, the number of binding sites per lipid, and the total lipid concentration, respectively. The parameter ε is defined as $\lambda_{max_o}/\lambda_{max}$. The parameter ε_b is a constant characteristic of a membrane-bound peptide and equals ε at a saturating lipid concentration when all of the peptide molecules present in the suspension are bound to the vesicles. According to equation 1, plotting $(\varepsilon - 1)$ versus $(\varepsilon - 1)/m$ gives K_d/n as the slope. K_d/n is used to compare pediocin PA-1 and its fragments with respect to their affinities for lipid vesicles.

Influence of pH on pediocin fragment binding. To determine the influence of pH on the binding of pediocin N15 and pediocin N8-15, large unilamellar vesicles were prepared at pH 6.0, 6.5, or 7.0 in 50 mM MES buffer and at pH 7.5 or 8.0 in 50 mM *N*-2-hydroxyethylpiperazine-*N*′-2-ethanesulfonic acid (HEPES) buffer. Fluorescence measurements were carried out in the buffer used to prepare lipid vesicles. Emission spectra were analyzed to determine the maximum increase in intensity at each pH. The net charge of pediocin N15 at each pH was calculated according to the amino acid sequence, assuming that the pKa values for α-COOH, α-NH_3^+, Lys^+, and His^+ were 3.5, 7.5, 10.4, and 6.5, respectively (11). The correlation between I_{max}/I_o and net positive charge of the peptide was examined. I_{max} was the value of I in the presence of saturating lipid concentration.

Quenching of tryptophan fluorescence by acrylamide. Native pediocin PA-1 contains two tryptophan residues, at positions 18 and 33. Acrylamide readily quenches tryptophan fluorescence in aqueous buffer (6, 9, 27). If the tryptophans penetrate into the hydrophobic phase of the lipid bilayer as a consequence of pediocin PA-1 binding to the lipid vesicles, the sensitivity of tryptophan fluorescence to the aqueous quencher decreases. To determine whether the two tryptophans bind to the lipid vesicles in a similar fashion, increasing amounts of a freshly prepared acrylamide stock solution (6 M) were added to a 3.8 μM pediocin PA-1 solution in the absence of lipid vesicles or in the presence of lipid vesicles at a ratio of lipid concentration to peptide concentration of about 150. Fluorescence measurements were carried out as described above. Fluorescence spectra were corrected for baseline levels measured with suspensions containing lipid vesicles plus appropriate amounts of acrylamide in MES buffer, and intensities were corrected for dilution effects. Quenching data were plotted as F_o/F

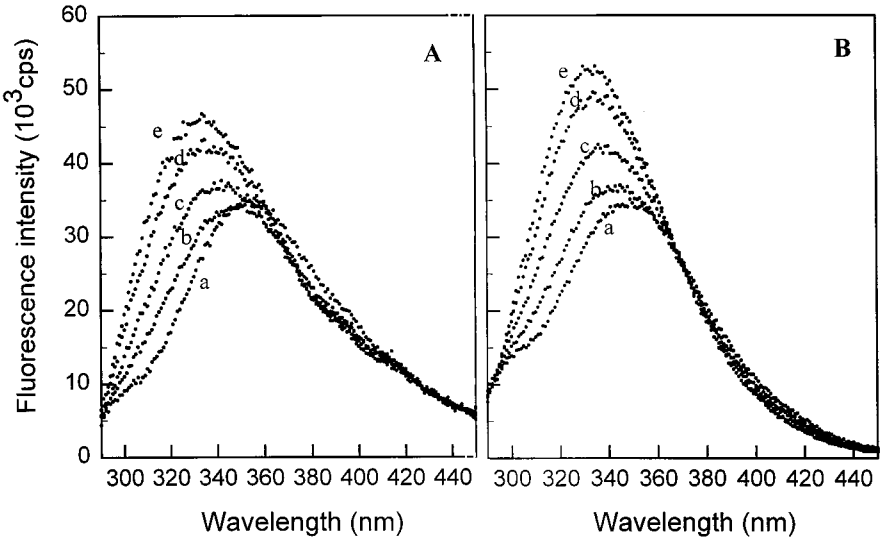

FIG. 1. Pediocin PA-1 (A) and pediocin N15 (B) binding to anionic lipid vesicles as demonstrated by an increase in *I* and a shift of the emission maximum to a lower wavelength. The pediocin PA-1 and pediocin N15 concentrations were 3.8 and 10.1 μM, respectively. In panel A, the lipid concentrations were 0, 21.1, 49.2, 104.9, and 214.7 μM for spectra a through e, respectively. In panel B, the lipid concentrations were 0, 7.1, 21.1, 49.2, and 104.9 μM for spectra a through e, respectively.

versus acrylamide concentration ([*Q*]), where F_o and *F* were the fluorescence intensities (of the whole emission spectrum) in the absence and presence of the quencher, respectively. The quenching plots were analyzed by using the following equations (6):

$$F_o/F = (1 + K_{sv}[Q])\exp(V[Q]) \quad (2)$$

for plots showing upward curvature, and

$$F_o/F = (1 + K_{sv}[Q]) \quad (3)$$

for straight plots, where *V* is a static quenching constant and K_{sv} is the Stern-Volmer quenching constant, which provides a basis for comparing the accessibility of the quencher to the tryptophan residues. The two-component dynamic quenching equation (6),

$$F/F_o = f_1/(1 + K_{sv,1}[Q]) + (1 - f_1/(1 + K_{sv,2}[Q]) \quad (4)$$

was used for plots showing downward curvature when we thought that the two tryptophan residues in the pediocin PA-1 sequence might localize differently in the lipid bilayer upon binding. $K_{sv,1}$ and $K_{sv,2}$ are the K_{sv} values for the two tryptophan residues. The nonlinear plots were analyzed by using the fitting program NFIT, version 1.0 (Island Products, Galveston, Tex.).

Carboxyfluorescein leakage assays. To determine whether the pediocin fragments permeablize lipid vesicles or compete with pediocin PA-1 for similar binding sites on the membrane surface, the carboxyfluorescein leakage assay was performed. The use of pediocin PA-1-mediated 5(6)-carboxyfluorescein (CF) efflux from *Listeria* lipid vesicles as a measure of pore formation activity is described elsewhere (8). Briefly, CF-loaded lipid vesicles were treated with pediocin N15 alone, with pediocin PA-1 alone, or with pediocin N15 for 1 min before pediocin PA-1 was added. Fluorescence intensity was recorded before and after the addition of the peptides. Complete CF release was determined by adding 0.2% (vol/vol) (final concentration) Triton X-100. The progress of CF efflux was calculated with the following equation: (% of CF efflux) = $[(F_t - F_o)/(F_\infty - F_o)]100$, where F_t was the fluorescence at time *t*, F_o was the baseline fluorescence for CF-loaded vesicles without added peptides, and F_∞ was the maximum fluorescence (100%) after Triton X-100 treatment.

Reagents. Culture media were obtained from Difco Laboratories (Detroit, Mich.). Acrylamide (electrophoresis grade), *N*-acetyltryptophanamide, and CF were obtained from Sigma Chemical Co. (St. Louis, Mo.). All other reagents, unless otherwise specified, were purchased from Fisher Scientific Co. (Pittsburgh, Pa.).

RESULTS AND DISCUSSION

Pediocin PA-1 binding to lipid vesicles probed by tryptophan fluorescence. Binding of pediocin PA-1 to the membrane was followed by determining the changes in the tryptophan fluorescence parameters, *I* and λ_{max}, when large unilamellar vesicles were added to a pediocin PA-1 solution. The emission spectrum of pediocin PA-1 in buffer (3.8 μM peptide in MES buffer, pH 6.0) had a maximum emission wavelength of 353 nm (Fig. 1A, spectrum a). This value is characteristic of the tryptophan residue fluorescence emission peak in aqueous solutions (38) and is within the same range as the values reported for pentagastrin-related pentapeptides (39) and a synthetic model peptide which has random structures in buffer but a β-structure in the presence of acidic lipid vesicles (25). A tryptophan derivative, *N*-acetyltryptophanamide, which mimics the tryptophan residue in a peptide but is always exposed to the aqueous solvent, had a λ_{max} of 357 nm in the MES buffer (data not shown). The smaller λ_{max} for pediocin PA-1 implies that, compared to the single-residue compound *N*-acetyltryptophanamide, the peptide with multiple amino acid residues may partially shield the residues from the aqueous solvent.

Upon addition of the lipid vesicles, the emission intensity increased slightly and the λ_{max} shifted to a lower (blue) wavelength (Fig. 1A, spectrum b). As more lipid vesicles were added (spectra c through e), *I* increased more and more, and λ_{max} shifted further toward the blue end of the spectrum. The decreases in λ_{max} and increases in *I* reflected the translocation of the tryptophan(s) in pediocin PA-1 from a hydrophilic, polar environment to a hydrophobic, nonpolar environment (24). These data demonstrated that pediocin PA-1 became bound to the lipid vesicles and that the tryptophan residue(s) penetrated into the hydrophobic phase of the lipid bilayer.

Pediocin PA-1 binding revealed by fluorescence quenching. An alternative approach to determine the binding state of pediocin PA-1 molecules involved the fluorescence quencher acrylamide. Acrylamide quenches the *I* of tryptophan residues exposed to aqueous phases, but it cannot access the residues in the interior of a folded protein or those buried in the membrane (6). The tryptophan fluorescence in pediocin PA-1 was quenched readily in MES buffer (Fig. 2). The Stern-Volmer plot for pediocin PA-1 in the absence of lipid vesicles had upward curvature, indicating that acrylamide was quenched by a static process as well as by the standard dynamic, or collisional, process (14). These data are similar to those reported by Chikindas et al. (9). In agreement with the characteristic λ_{max}, the quenching data suggest that both tryptophan residues

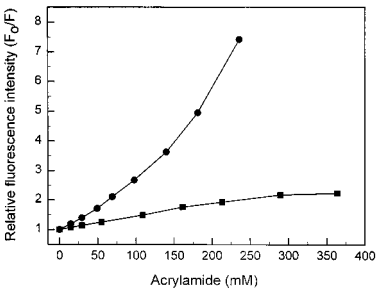

FIG. 2. Quenching of pediocin PA-1 tryptophan fluorescence as a function of acrylamide concentration in the absence of lipids (●) and in the presence of 638 μM lipid vesicles (■). The pediocin PA-1 concentration was 3.8 μM. Data points were connected with lines (i.e., the lines are not the results of curve fitting).

TABLE 2. Binding parameters of peptide-lipid complexes for pediocin PA-1 and pediocin fragments[a]

Peptide	$\Delta\lambda_{max}$ (nm)[b]	K_d/n (mM)
Pediocin PA-1	20.5 ± 0.7	0.039 ± 0.008
Pediocin N15	17.7 ± 0.7	0.028 ± 0.006
Pediocin N8-15	14.5 ± 0.5	0.089 ± 0.021
Pediocin N7	11.0 ± 0.6	0.36 ± 0.012
Pediocin N^m8-15	0	NA[c]

[a] Means and standard errors were obtained from three independent experiments for each peptide. For K_d/n calculations with equation 1, the parameter ε was defined as the relative blue shift (i.e., $\lambda_{max_0}/\lambda_{max}$).

[b] Maximum blue shift in λ_{max} obtained for each peptide in the presence of a saturating amount of lipid vesicles.

[c] NA, equation 1 could not be applied to an ε value of 1 ($\Delta\lambda_{max} = 0$).

of pediocin PA-1 are highly exposed to the aqueous buffer in the absence of lipid vesicles. In contrast, quenching was significantly less in the presence of the lipid vesicles at a ratio of lipid concentration to peptide concentration of 168, a saturating level of lipid vesicles (saturation of pediocin binding occurred at a ratio of lipid concentration to peptide concentration of 60 [see below]). For example, acrylamide at a concentration of about 230 mM quenched the tryptophan fluorescence of pediocin PA-1 in buffer by sevenfold but quenched the tryptophan fluorescence of pediocin PA-1 in the presence of the lipid vesicles by only twofold. These data further confirmed that the tryptophan residue(s) had translocated into a nonpolar, hydrophobic environment and that pediocin PA-1 had bound to the anionic lipid vesicles.

Analysis of the Stern-Volmer plots gave a K_{sv} of 8.83 ± 0.42 M^{-1} and a V of 2.93 ± 0.42 M^{-1} for pediocin PA-1 in buffer alone (as determined with equation 2) and a K_{sv} of 3.53 ± 0.67 M^{-1} for the bacteriocin bound to the lipid vesicles (as determined with equation 3, for $[Q] < 250$ mM). Three independent experiments were done to obtain data for the K_{sv} calculation, and Fig. 2 shows a representative set of data. The K_{sv} for bound pediocin PA-1 was more than two times less than the quenching constant for pediocin PA-1 in buffer, suggesting that pediocin molecules were inserted into the anionic phospholipid vesicles. Furthermore, the Stern-Volmer plot for the bound pediocin PA-1 tended to plateau at acrylamide concentrations higher than 250 mM (Fig. 2). This implied that the two tryptophan residues of the membrane-bound pediocin molecules had different accessibilities to the quencher. Analyzing the Stern-Volmer plots for quenching in the presence of lipid vesicles by using the two-component dynamic quenching equation (equation 4) resulted in a $K_{sv,1}$ of zero and a $K_{sv,2}$ of 8.85 ± 0.71 M^{-1}. These quenching constants strongly suggested that differentiated binding of the two tryptophan residues occurred; one tryptophan (with a K_{sv} of zero) was buried deeply in the hydrophobic core of the lipid bilayer and was inaccessible, while the other tryptophan (with a K_{sv} that was the same as the K_{sv} in buffer) was located at the membrane surface and was thus essentially exposed to solvent for quenching by acrylamide. Unlike iodide (I^-), which is repelled by negatively charged phospholipid head groups, acrylamide bears no charge and can diffuse to the surface of the anionic lipid bilayer and contact the surface-bound tryptophan residue when it has not penetrated the bilayer.

Quenching of tryptophan fluorescence in nisin I30W by iodide (I^-) and in pediocin PA-1 by acrylamide was studied previously (9, 27), but no quenching constant was reported. The K_{sv} for pediocin PA-1 in buffer solution is similar to the K_{sv} reported for tryptophan residues in a coiled-coil protein, the myosin rod, which has a K_{sv} of 8.4 M^{-1} for monomers (6). Nisin I30W binds to and inserts into lipid vesicles consisting of phosphatidylcholine-phosphatidylethanolamine and of phosphatidylcholine-cardiolipin. The negatively charged cardiolipin deepens the location of the tryptophan residue in the hydrophobic core of the lipid bilayer, and insertion of nisin is more extensive (27). Chikindas et al. (9) reported that pediocin PA-1 binds to *Escherichia coli* lipid vesicles having a high content of zwitterionic phospholipids (42). Upon association of pediocin PA-1 with zwitterionic lipid vesicles, the tryptophan residues are located on the surface of the bilayer (9). In the presence of the anionic lipid vesicles, this study shows that the quenching of pediocin PA-1 fluorescence by acrylamide was significantly less than the quenching in the presence of *E. coli* lipid vesicles, and the two-component analysis suggested that one of the tryptophan residues was preferentially inserted into the anionic membranes. Whether interaction of pediocin PA-1 with the anionic lipid vesicles causes a conformational change within the pediocin molecule has yet to be determined. Lipid-induced conformational change per se could result in a more nonpolar environment for the tryptophan residues of pediocin PA-1 (9). However, the more extensive blue shift in λ_{max} (more than 20 nm) (Table 2) and the increases in I upon interaction with the anionic lipid vesicles compared to the results obtained for the interaction of pediocin PA-1 with *E. coli* lipid vesicles could not be attributed to conformational changes alone. Therefore, membrane insertion of pediocin PA-1 played a major role in the observed changes in fluorescence parameters in the presence of the anionic phospholipid vesicles.

Pediocin N15 binding: comparison with pediocin PA-1 binding. To test the hypothesis that the N terminus and the positive patch at the tip of the hairpin loop predicted by the pediocin PA-1 structural model (8) were involved in binding, we examined the binding of the fragment pediocin N15 (derived from the first 15 residues of pediocin PA-1; Table 1) as well as three other fragments, to the anionic lipid vesicles (see below).

Like pediocin PA-1, pediocin N15 bound to the anionic lipid vesicles (Fig. 1B). As progressively higher concentrations of vesicles were added to a pediocin N15 solution (10.1 μM, pH 6.0), there was a greater blue shift in λ_{max} and a greater increase in I. This indicated that progressively more pediocin N15 molecules became bound to the membrane. Similar changes in the emission maximum were observed for the native bacteriocin and the fragment (Fig. 3); for both peptides, addition of anionic lipid vesicles caused an increase in the magnitude of the blue shift of λ_{max}. At a certain lipid concentration, all peptides became bound, and the curves plateaued. Pediocin PA-1 binding reached saturation at a ratio of lipid concentra-

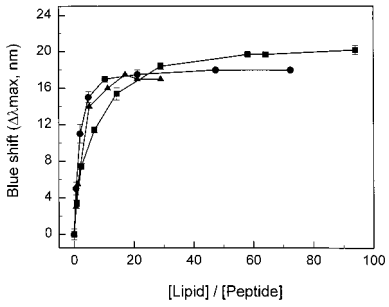

FIG. 3. Binding titration curves for binding of 3.8 μM pediocin PA-1 (■) and 10.1 μM pediocin N15 (●) to anionic lipid vesicles and for binding of 10.1 μM pediocin N15 (▲) to lipid vesicles derived from *L. monocytogenes*. The means and standard errors involving the anionic lipid vesicles were from three independent experiments, and the results involving the *Listeria* lipid vesicles were the averages from two experiments.

tion to lipid peptide concentration of about 60. Saturation for pediocin N15 was reached at a ratio of about 20. The difference can be explained by the bigger size of the native peptide, which consisted of 44 amino acids, compared to the 15-amino-acid fragment, since the two peptides showed similar abilities to bind to membranes (see below).

Pediocin N15 did not kill *L. monocytogenes* Scott A (data not shown), probably because it is too short to form functioning pores in the membrane. Pediocin N15 alone did not cause CF efflux from *Listeria* lipid vesicles (Fig. 4). As a control, the full-length molecule pediocin PA-1 induced CF efflux as expected. When CF-loaded lipid vesicles were treated with pediocin N15 prior to the addition of pediocin PA-1, the onset of CF efflux was delayed. Since pediocin PA-1 and pediocin N15 are both positively charged in the buffer and the fragment is largely hydrophilic, they are more likely to repel than to interact with each other in the solution. On the other hand, both peptides have a strong tendency to interact with the membrane. Pediocin N15 bound as strongly as pediocin PA-1 did to the anionic lipid vesicles (see below) (Table 2), and it bound to *Listeria* lipid vesicles like it bound to anionic lipid vesicles (Fig. 3). In their membrane-bound states, the pediocin fragment might interact with the full-length peptide to form nonfunctioning pores, as proposed for the antagonistic effect of nisin[1-12] on full-length nisin (5); however, this does not explain the delayed onset of efflux. A more plausible explanation is that pediocin N15 competed with pediocin PA-1 for the same binding sites on the *Listeria* lipid vesicles. Probably due to better insertion (see below) and pore-forming ability, the native peptide eventually displaced the bound fragment and permeabilized the lipid vesicles.

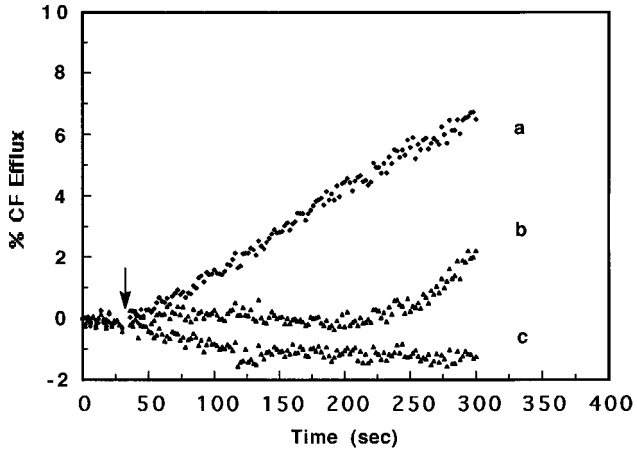

FIG. 4. CF efflux from *Listeria* lipid vesicles induced by pediocin PA-1 and pediocin N15. Efflux a, pediocin PA-1 (1.5 μM); efflux b, pediocin N15 (1.7 μM) and pediocin PA-1 (1.5 μM); efflux c, pediocin N15 (1.7 μM). See Materials and Methods for details.

Taken together, the similar fluorescence titration curves displayed by pediocin N15 and pediocin PA-1 (Fig. 3) and the possible competition between the two peptides for similar binding sites on *Listeria* lipid vesicles (Fig. 4) demonstrate that pediocin N15 and the complete, native bacteriocin bind to membranes in similar manners. Therefore, the fragment binding kinetics provides a suitable model for the binding of pediocin PA-1. The fact that pediocin N15 bound similarly to *Listeria* lipid vesicles and to anionic lipid vesicles further supports the appropriateness of the anionic lipid model.

Binding of pediocin fragments: the role of positively charged residues. To examine how different domains of pediocin N15 contribute to binding, two small fragments, pediocin N7 and pediocin N8-15 (Table 1), were exposed to lipid vesicles, and their fluorescence emission spectra were determined. Pediocin N8-15 bound to the lipid vesicles like pediocin N15 bound to lipid vesicles, but there were marked differences with pediocin N7 (spectral data not shown). Further analysis of the emission spectra for pediocin N15, pediocin N7, and pediocin N8-15 obtained in the presence of lipids resulted in three types of binding curves (Fig. 5). The binding of the pediocin fragments was plotted as the blue shift in λ_{max} (Fig. 5A), the relative blue shift ($\lambda_{max_o}/\lambda_{max}$) (Fig. 5B), or the relative intensity increase (I/I_o) (Fig. 5C) versus the total lipid concentrations. All three types of titration curves indicate the extent of binding for a peptide.

For pediocin N15, whose binding behavior is comparable to that of pediocin PA-1 (Fig. 3), increasing the concentration of lipid vesicles increased both the extent of the blue shift (Fig. 5A and B, line a) and the relative intensity (Fig. 5C, line a). Pediocin N7, which does not contain the positive patch but does contain the YGNGV consensus motif, which is thought to be the *Listeria* recognition site for class IIa bacteriocins (2, 4, 23), bound only weakly to the phospholipid vesicles. The small extent of the blue shift observed for pediocin N7 (Fig. 5A and B, line c) did not take place until the lipid concentration was about 100 μM, a concentration at which the majority of pediocin N15 was bound. Saturation of pediocin N7 binding also required a much higher lipid concentration than did saturation of pediocin N15 binding. In contrast to pediocin N7, pediocin N8-15 (containing the positive patch) bound more strongly to the lipid vesicles, and the lipid dependence of the blue shift (Fig. 5A and B, line b) and the relative intensity increase (Fig. 5C, line b) was more similar to that for pediocin N15. These data suggested that it was the positive patch rather than the YGNGV consensus motif that was responsible for the initial binding of the pediocin fragments. To test this hypothesis, the positive patch was mutated out of pediocin N8-15, and binding was examined. The mutated fragment pediocin N^m8-15, which contained no charged residues (Lys-11 and His-12 were replaced with Ile-11 and Leu-12), did not bind at pH 6.0 (Fig. 5, lines d). For pediocin N^m8-15, addition of as many lipid vesicles as were added for pediocin N8-15 did not cause either an increase in relative intensity or a blue shift of λ_{max}. Therefore, removing the positive patch eliminated binding. Modifying the charge of pediocin N8-15 by changing the pH resulted in a similar effect. When the anionic lipid vesicles prepared at pH 8.0 were added to pediocin N8-15 in HEPES buffer at pH 8.0,

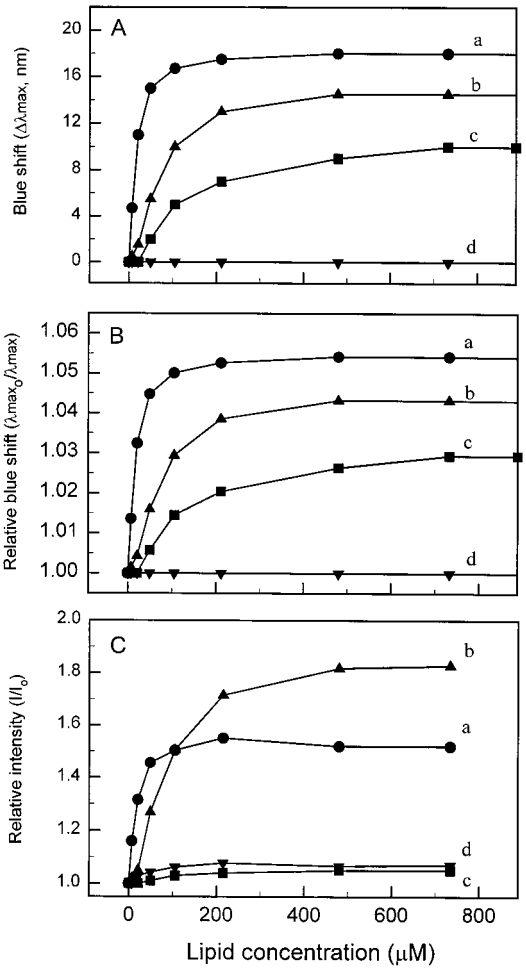

FIG. 5. Binding titration curves for pediocin fragments, expressed as the curves for the blue shift in maximum emission wavelength (A), the relative blue shift (B), and the relative intensity increase (C). Symbols: ●, pediocin N15 (10.1 μM); ■, pediocin N7 (10.5 μM); ▲, pediocin N8-15 (11.0 μM); ▼, pediocin N^{m}8-15 (7.2 μM).

there was no blue shift in λ_{max}, and the *I* decreased slightly due to dilution effect (data not shown), indicating that no binding occurred at pH 8.0. These results demonstrate that electrostatic interactions, but not the YGNGV consensus motif, govern the initial binding of the pediocin fragments to the anionic phospholipid vesicles. This is consistent with the initial incorporation of nisin into artificial lipid vesicles, which is enhanced by electrostatic interactions between positively charged nisin molecules and negatively charged phospholipid head groups of vesicles (27).

On the basis of a comparison of the activities of chemically synthesized class IIa bacteriocins and their hybrids against various indicator strains, Fimland et al. (15) suggested that the C-terminal parts of pediocin-like bacteriocins, including the C-terminal part of pediocin PA-1, play an important role in membrane interaction and target cell specificity. Results from the present study show that the N-terminal part of pediocin PA-1 also binds to the target membrane. The binding of the N-terminal part not only may contribute to the overall interaction of the pediocin molecule with the target membrane, but also may make it possible for the C-terminal part of the sequence to assume a defined secondary structure. The C-terminal parts of pediocin-like bacteriocins may exist as random coils in aqueous solutions, as predicted by computer modeling of pediocin PA-1 (8) and demonstrated by a nuclear magnetic resonance study of leucocin A (37). The C-terminal section of leucocin A has an α-helical structure only in membrane-mimicking environments, such as trifluoroethanol or dodecyl phosphocholine micelles. Electrostatic interactions are responsible for the initial binding of pediocin PA-1 and other pediocin-like bacteriocins to target membranes. The specificity and potency of the bacteriocin may be determined by the amphiphilic nature of the resultant secondary structure in the C-terminal part (15) and to other factors, such as the membrane composition of the target cell. Specificity and potency may be attributed, at least in part, to the content of negatively charged lipids in the target membrane, which influences the degree of electrostatic interactions.

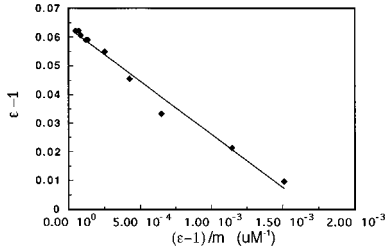

FIG. 6. Generation of a binding parameter for pediocin PA-1. K_d/n is the slope of the fitted line as determined with equation 1 (see text for details).

Binding parameters of pediocin peptides: comparison of affinity and degree of insertion. To obtain dissociation constants, the binding titration curves for pediocin PA-1 (Fig. 3) and its fragments (Fig. 5B) were analyzed by using equation 1. Briefly, the curve for pediocin PA-1 in Fig. 3 was replotted as $\lambda_{max_o}/\lambda_{max}$ versus *m* to form a curve which resembles the curves in Fig. 5B. As mentioned above, ε is defined as $\lambda_{max_o}/\lambda_{max}$; for pediocin PA-1, λ_{max_o} was 353 nm, and λ_{max} was calculated by subtracting $\Delta\lambda_{max}$ from λ_{max_o}. The next step was to calculate and plot $(\varepsilon - 1)$ versus $(\varepsilon - 1)/m$ and to fit the data points with equation 1 (Fig. 6). The slope of the straight line is K_d/n, i.e., K_d normalized to *n*. The data for pediocin fragments were analyzed in the same manner (data not shown).

The binding parameters for each peptide at pH 6.0 are shown in Table 2. A smaller K_d/n indicates that a peptide has a stronger affinity for the membrane (3, 25, 27, 39). The K_d/n values for pediocin PA-1 and pediocin N15 were similar, indicating that they have similar relative affinities for the anionic lipid vesicles. This confirmed the comparable membrane binding behaviors of pediocin N15 and pediocin PA-1. On the other hand, the relative affinity of pediocin N8-15 for the anionic lipid vesicles was two times lower than that of pediocin N15, and dramatically, the relative affinity of pediocin N7 was lower by an order of magnitude (K_d/n was 10-fold higher).

The maximum blue shift ($\Delta\lambda_{max}$) was also lower for the two smaller fragments compared to pediocin PA-1 and pediocin N15 (Table 2). Comparison of the K_d/n values and the $\Delta\lambda_{max}$ values suggested that there is a correlation between binding and blue shift; the tighter a peptide bound to the lipid vesicles (with a smaller K_d/n), the greater the $\Delta\lambda_{max}$. A higher value for $\Delta\lambda_{max}$ indicates a more hydrophobic environment for the tryptophan residue as a consequence of membrane binding and insertion. The largest $\Delta\lambda_{max}$ for pediocin PA-1 suggested that the most extensive insertion of the tryptophan residues occurred with the complete peptide. In contrast, the tryptophan residue in membrane-bound pediocin N7 is located in a less

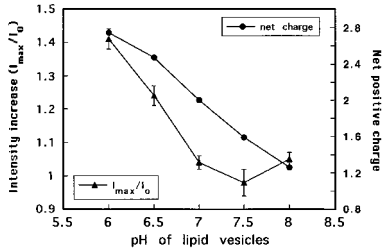

FIG. 7. Influence of pH on ionization state and binding of pediocin N15. The peptide concentration was 8.5 μM, and the lipid concentration was 480 μM. See Materials and Methods for details.

hydrophobic environment, suggesting that the lowest degree of membrane insertion occurs. It appeared that the extent of membrane insertion modulated the binding affinity of the peptide. Deeper insertion of the peptide might cause a decreased rate of dissociation of the bound peptide from the lipid vesicles, thus increasing the binding affinity.

At pH 6.0, the numbers of positive charges (indicated in parentheses) for the peptides are pediocin PA-1 (8) > pediocin N15 (4) > pediocin N8-15 (3) > pediocin N7 (2). Pediocin N^m8-15, which contains one positive charge (α-NH_3^+), showed no change in $\Delta\lambda_{max}$, and no binding parameter could be calculated. The binding affinity of pediocin PA-1 and its fragments toward the anionic lipid vesicles correlated well with the number of positive charges in the peptide.

Influence of pH on pediocin N15 binding. Additional evidence supporting the electrostatic interaction model was obtained by studying changes in pediocin N15 fluorescence emission during gradual changes in the pH of buffer containing vesicles. The net positive charge of pediocin N15 decreased as the pH increased from 6.0 to 8.0 (Fig. 7). Considering all of the charged groups on the fragment, it has a net positive charge of +2.8 at pH 6.0 and of +1.3 at pH 8.0. Increasing the pH deprotonated the His residue and the α-amino group, while other charged groups were not significantly modified. Binding of pediocin N15 to the lipid vesicles at pH 6.0 caused a 41% ± 3% increase in *I*. At pH 6.5, the increase was 24% ± 3%, and at pH 7.0 it was 4% ± 2%. Little increase in intensity was observed at pH 7.5 and 8.0. The influence of pH on the blue shift in λ_{max} followed a similar pattern (data not shown), with gradual drops in magnitude from pH 6.0 to 7.0 and significant drops from pH 7.0 to 8.0. The enhanced pediocin N15 binding at acidic pH paralleled the net positive charge on the fragment. This is consistent with the modulating effect of pH on permeabilization of *Listeria* lipid vesicles by pediocin PA-1, where the CF efflux rate also parallels the net positive charge in the complete peptide (8).

Conclusions. We used intrinsic tryptophan fluorescence to investigate the binding of pediocin PA-1 and its fragments to target membranes. We found that the mechanism for the initial binding step primarily involves electrostatic interactions between positive patches of amino acid residues in the pediocin molecules and negatively charged phospholipid head groups in the target membrane. The YGNGV consensus motif does not appear to be involved in this initial binding step. This study provides new insights into the mechanism of pediocin PA-1 action which could be useful for genetic engineering of pediocin PA-1 variants with improved potency. With respect to food preservation, pediocin PA-1 and low pH can work synergistically to inhibit food-borne pathogens because low pH should both stress the target pathogen and strengthen pediocin PA-1's action by increasing its net positive charge. In addition, pediocin PA-1 may work better in low-salt (low-ionic-strength) than in high-salt food systems because a high ionic strength should weaken the electrostatic interactions.

ACKNOWLEDGMENTS

Research in our laboratory and preparation of the manuscript were supported by state appropriations, by U.S. Hatch Act funds, and by the U.S.-Israel Binational Agricultural Research and Development Fund (grant US-2113-92).

We thank K. Schaich for the use of instruments in her laboratory and Z. Rajfur for assistance with spectrofluorometer operation.

REFERENCES

1. **Abee, T.** 1995. Pore-forming bacteriocins of Gram-positive bacteria and self-protection mechanisms of producer organisms. FEMS Microbiol. Lett. **129:**1–10.
2. **Abee, T., L. Krockel, and C. Hill.** 1995. Bacteriocins: modes of action and potentials in food preservation and control of food poisoning. Int. J. Food Microbiol. **28:**169–185.
3. **Bashford, C. L., B. Chance, J. C. Smith, and T. Yoshida.** 1979. The behavior of oxonol dyes in phospholipid dispersions. Biophys. J. **25:**63–85.
4. **Bhugaloo-Vial, P., X. Dousset, A. Metivier, O. Sorokine, P. Anglade, P. Boyaval, and D. Marion.** 1996. Purification and amino acid sequences of piscicocins V1a and V1b, two class IIa bacteriocins secreted by *Carnobacterium piscicola* V1 that display significantly different levels of specific inhibitory activity. Appl. Environ. Microbiol. **62:**4410–4416.
5. **Chan, W. C., M. Leyland, J. Clark, H. M. Dodd, L.-Y. Lian, M. J. Gasson, B. W. Bycroft, and G. C. K. Roberts.** 1996. Structure-activity relationships in the peptide antibiotic nisin: antimicrobial activity of fragments of nisin. FEBS Lett. **390:**129–132.
6. **Chang, Y.-C., and R. D. Ludescher.** 1994. Local conformation of rabbit skeletal myosin rod filaments probed by intrinsic tryptophan fluorescence. Biochemistry **33:**2313–2321.
7. **Chen, Y., and T. J. Montville.** 1995. Efflux of ions and ATP depletion induced by pediocin PA-1 are concomitant with cell death in *Listeria monocytogenes* Scott A. J. Appl. Bacteriol. **79:**684–690.
8. **Chen, Y., R. Shapira, M. Eisenstein, and T. J. Montville.** 1997. Functional characterization of pediocin PA-1 binding to liposomes in the absence of a protein receptor and its relationship to a predicted tertiary structure. Appl. Environ. Microbiol. **63:**524–531.
9. **Chikindas, M. L., M. J. Garcia-Garcera, A. J. M. Driessen, A. M. Ledeboer, J. Nissen-Meyer, I. F. Nes, T. Abee, W. N. Konings, and G. Venema.** 1993. Pediocin PA-1, a bacteriocin from *Pediococcus acidilactici* PAC 1.0, forms hydrophilic pores in the cytoplasmic membrane of target cells. Appl. Environ. Microbiol. **59:**3577–3584.
10. **Crandall, A. D.** 1997. Resistance to the bacteriocin nisin in *Listeria monocytogenes*. Ph.D. dissertation. Rutgers, The State University of New Jersey, New Brunswick.
11. **Creighton, T. E.** 1993. Chemical properties of polypeptides, p. 1–47. *In* Proteins: structures and molecular properties, 2nd ed. Freeman and Company, New York, N.Y.
12. **Demel, R. A., T. Peelen, R. J. Siezen, B. de Kruijff, and O. P. Kuipers.** 1996. Nisin Z, mutant nisin Z and lacticin 481 interactions with anionic lipids correlate with antimicrobial activity. A monolayer study. Eur. J. Biochem. **235:**267–274.
13. **Driessen, A. J. M., H. W. van den Hooven, W. Kuiper, M. van de Kamp, H.-G. Sahl, R. N. H. Konings, and W. N. Konings.** 1995. Mechanistic studies of lantibiotic-induced permeabilization of phospholipid vesicles. Biochemistry **34:**1606–1614.
14. **Eftink, M. R.** 1991. Fluorescence quenching: theory and applications, p. 53–127. *In* J. R. Lakowicz (ed.), Topics in fluorescence spectroscopy, vol. 2. Principles. Plenum Press, New York, N.Y.
15. **Fimland, G., O. R. Blingsmo, K. Sletten, G. Jung, I. F. Nes, and J. Nissen-Meyer.** 1996. New biologically active hybrid bacteriocins constructed by combining regions from various pediocin-like bacteriocins: the C-terminal region is important for determining specificity. Appl. Environ. Microbiol. **62:**3313–3318.
16. **García-Garcerá, M. J., M. G. L. Elfernic, A. J. M. Driessen, and W. N. Konings.** 1993. In vitro pore-forming activity of the lantibiotic nisin: role of the proton motive force and lipid composition. Eur. J. Biochem. **212:**417–422.
17. **Giffard, C. J., H. M. Dodd, N. Horn, S. Ladha, A. R. Mackie, A. Parr, M. J. Gasson, and D. Sanders.** 1997. Structure-function relations of variant and fragment nisin studied with model membrane systems. Biochemistry **36:** 3802–3810.
18. **Giffard, C. J., S. Ladha, A. R. Mackie, D. C. Clark, and D. Sanders.** 1996. Interaction of nisin with planar lipid bilayers monitored by fluorescence recovery after photobleaching. J. Membr. Biol. **151:**293–300.
19. **Gonzalez, C. F.** December 1988. Method for inhibiting bacterial spoilage and

composition for this purpose. European patent application 88101624.
20. **Henderson, J. T., A. L. Chopko, and P. D. van Wassenaar.** 1992. Purification and primary structure of pediocin PA-1 produced by *Pediococcus acidilactici* PAC-1.0. Arch. Biochem. Biophys. **295:**5–12.
21. **Hurst, A.** 1981. Nisin. Adv. Appl. Microbiol. **27:**85–123.
22. **Jack, R. W., J. R. Tagg, and B. Ray.** 1995. Bacteriocins of gram-positive bacteria. Microbiol. Rev. **59:**171–200.
23. **Klaenhammer, T. R.** 1993. Genetics of bacteriocins produced by lactic acid bacteria. FEMS Microbiol. Rev. **12:**39–86.
24. **Lakowicz, J. R.** 1983. Principles of fluorescence spectroscopy. Plenum Press, New York, N.Y.
25. **Lee, S., T. Iwata, H. Oyagi, H. Aoyagi, M. Ohno, K. Anzai, Y. Kirino, and G. Sugihara.** 1993. Effect of salts on conformational change of basic amphipathic peptides from β-structure to α-helix in the presence of phospholipid liposomes and their channel-forming ability. Biochim. Biophys. Acta **1151:** 76–82.
26. **MacDonald, R. C., R. I. MacDonald, B. P. M. Menco, K. Takeshita, N. K. Suddarao, and L. Hu.** 1991. Small-volume extrusion apparatus for preparation of large, unilamellar vesicles. Biochim. Biophys. Acta **1061:**297–303.
27. **Martin, I., J.-M. Ruysschaert, D. Sanders, and C. J. Giffard.** 1996. Interaction of the lantibiotic nisin with membranes revealed by fluorescence quenching of an introduced tryptophan. Eur. J. Biochem. **239:**156–164.
28. **Matsuzaki, K., O. Murase, H. Tokuda, S. Funakoshi, N. Fujii, and K. Miyajima.** 1994. Orientational and aggregational states of magainin 2 in phospholipid bilayers. Biochemistry **33:**3342–3349.
29. **Mazzotta, A., and T. J. Montville.** 1997. Nisin induces changes in membrane fatty acid composition of *Listeria monocytogenes* nisin-resistant strains at 10°C and 30°C. J. Appl. Microbiol. **82:**32–38.
30. **McMullen, L. M., L. Saucier, J. L. Leisner, G. G. Greer, and M. E. Stiles.** 1995. Bacteriocinogenic activity of *Leuconostoc gelidum* UAL 187 in MAP fresh meat, abstr. P5. *In* Abstracts of the Workshop on the Bacteriocins of Lactic Acid Bacteria: Application and Fundamentals, Banff, Alberta, Canada.
31. **Montville, T. J., and K. Winkowski.** 1997. Biologically-based preservation systems and probiotic bacteria, p. 557–577. *In* M. P. Doyle, L. R. Beuchat, and T. J. Montville (ed.), Food microbiology: fundamentals and frontiers. American Society for Microbiology Press, Washington, D.C.
32. **Montville, T. J., K. Winkowski, and R. D. Ludescher.** 1995. Models and mechanisms for bacteriocin actions and application. Int. Dairy J. **5:**797–814.
33. **Nielsen, J. W., J. S. Dickson, and J. D. Crouse.** 1990. Use of bacteriocin produced by *Pediococcus acidilactici* to inhibit *Listeria monocytogenes* associated with fresh meat. Appl. Environ. Microbiol. **56:**2142–2145.
34. **Ojcious, D. M., and J. D. E. Young.** 1991. Cytoplasmic pore forming proteins and peptides: is there a common structural motif? Trends Biochem. Sci. **16:**225–229.
35. **Pucci, M. J., E. R. Vedamuthu, B. S. Kunka, and P. A. Vandenberg.** 1988. Inhibition of *Listeria monocytogenes* by using bacteriocin PA-1 produced by *Pediococcus acidilactici* PAC1.0. Appl. Environ. Microbiol. **54:**2349–2353.
36. **Sahl, H. G.** 1991. Pore formation in bacterial membranes by cationic lantibiotics, p. 347–358. *In* G. Jung and H. G. Sahl (ed.), Nisin and novel lantibiotics. Proceedings of the First International Workshop on Lantibiotics. ESCOM Science Publishers, Leiden, The Netherlands.
37. **Sailer, M., W. P. Niemczura, T. T. Nakashima, M. E. Stiles, and J. C. Vederas.** 1995. 3D structure of leucocin A in environments that mimic membranes, abstr. P23. *In* Abstracts of the Workshop on the Bacteriocins of Lactic Acid Bacteria: Applications and Fundamentals, Banff, Alberta, Canada.
38. **Strasbury, G. M., and R. D. Ludescher.** 1995. Theory and applications of fluorescence spectroscopy in food research. Trends Food Sci. Technol. **6:**69–75.
39. **Surewicz, W. K., and R. M. Epand.** 1984. Role of peptide structure in lipid-peptide interactions: a fluorescence study of the binding of pentagastrin-related pentapeptides to phospholipid vesicles. Biochemistry **23:**6072–6077.
40. **Vandenbergh, P. A., M. J. Pucci, B. S. Kunka, and E. R. Vedamuthu.** August 1989. Method for inhibiting *Listeria monocytogenes* using a bacteriocin. European patent application 89101125.6.
41. **Van Den Hooven, H. W., C. A. E. M. Sponk, M. Van De Camp, R. N. H. Konings, C. W. Hilbers, and F. J. M. Van De Ven.** 1996. Surface location and orientation of the lantibiotic nisin bound to membrane-mimicking micelles of dodecylphosphocholine and of sodium dodecylsulphate. Eur. J. Biochem. **235:**394–403.
42. **Wilkinson, S. G.** 1988. Gram-negative bacteria, p. 308–317. *In* C. Ratledge and S. G. Wilkinson (ed.), Microbial lipids, vol. I. Academic Press, San Diego, Calif.
43. **Winkowski, K., A. D. Crandall, and T. J. Montville.** 1993. Inhibition of *Listeria monocytogenes* by *Lactobacillus bavaricus* MN in beef systems at refrigeration temperatures. Appl. Environ. Microbiol. **59:**2552–2557.
44. **Winkowski, K., R. D. Ludescher, and T. J. Montville.** 1996. Physicochemical characterization of the nisin-membrane interaction with liposomes derived from *Listeria monocytogenes*. Appl. Environ. Microbiol. **62:**323–327.